

DYNAMIC COMPRESSION OF WET HANDSHEETS

Project 3258

**Report Three
A Progress Report
to**

MEMBERS OF THE INSTITUTE OF PAPER CHEMISTRY

September 15, 1977

THE INSTITUTE OF PAPER CHEMISTRY

Appleton, Wisconsin

DYNAMIC COMPRESSION OF WET HANDSHEETS

Project 3258

Report Three

A Progress Report

to

MEMBERS OF THE INSTITUTE OF PAPER CHEMISTRY

September 15, 1977

TABLE OF CONTENTS

	Page
SUMMARY	1
INTRODUCTION	2
EXPERIMENTAL	4
Apparatus	4
Procedure	4
STATIC COMPRESSION	7
Sheet	7
Felt	9
Sheet and Felt	10
DYNAMIC COMPRESSION IN THE PRESENCE OF A FELT	12
Applied Pressure	12
Hydraulic Pressure	15
Sheet Thickness	19
DYNAMIC COMPRESSION WITHOUT FELT	23
Pressure Schedule	23
Sheet Deformation	25
Hydraulic Pressure	29
Basis Weight	32
Pulp Refining	36
LITERATURE CITED	43

THE INSTITUTE OF PAPER CHEMISTRY

Appleton, Wisconsin

DYNAMIC COMPRESSION OF WET HANDSHEETS

SUMMARY

Dynamic compression of wet handsheets was tested in a platen press at different rates of pressure rise to a preset value. The handsheets were made of a northern bleached softwood kraft pulp. The data were reported in applied pressure, hydraulic pressure, and sheet thickness as functions of time. The test results were further correlated to show the effects of compression time, basis weight, and pulp refining on dewatering.

For a heavy sheet made of the disintegrated pulp with a high freeness (\sim CSF 700) the final sheet density or water content is governed by the sheet compressibility in longer times of compression and by the flow resistance in short times. A 400 g/m^2 sheet attained a dryness of 42% at a pressure of 4.8×10^7 dyne/cm² in 24 milliseconds. The dryness increased to 61% in 90 milliseconds. The same sheet reached 70% in 15 minutes at the pressure.

The test apparatus and procedure are suitable for determining the dynamic effects in rapid compression. The dynamic test will be useful for evaluating the performance of a transversal-flow press, the effects of operating parameters, and those of felts and chemical additives in dewatering.

INTRODUCTION

In the present state of wet pressing, the maximum web dryness attained in a press nip is not known. As reviewed in Report One, a high exit moisture may be a consequence of inadequate compression, excessive rewetting, or both. To investigate the dryness of paper and board attainable by compression alone, a platen press was constructed with well-defined boundaries and instrumented for rapid changes of applied pressure, material thickness, and hydraulic pressure.

The compression apparatus was used to test a thick, filtration-formed, water-saturated, and mechanically conditioned mat of dacron fibers. The test showed a thickness reduction by 27% as the applied pressure rose to 4×10^6 dynes per sq cm (≈ 60 psi) in the initial 0.04 second, during which the hydraulic pressure drop across the mat reached a peak of about 1.5×10^5 dyne/cm² in 0.025 sec and then decayed as rapidly. In Report Two, these results were compared with the computed solutions of a mathematical model developed at the Institute. The model is capable of predicting the thickness change, the hydraulic pressure history, and the instantaneous porosity distribution when the pressure schedule and the compressibility and permeability data are given. In comparison, the thickness predictions were 10-15% lower than the measured values; the predicted hydraulic pressure pattern resembled the recorded curve, the former, however, leading the latter by about 0.004 second. The discrepancies were attributed to the use of the static compressibility function in the model.

The compression of the highly permeable dacron mat was controlled by its compressibility, the effect of flow resistance being small. In the dynamic test, the viscoelastic fiber structure did not have enough time to respond to the rapidly rising pressure as much as in the static test at constant pressure.

Consequently, the predicted thickness was too low. In a nearly uniform mat, the hydraulic pressure drop necessary for the flow of water varies directly with the product of the rate of thickness reduction, the thickness itself, and the flow resistance which is a strong function of the thickness. The delayed response of deformation would be reflected in the generation of hydraulic pressure. The predictions based on the instantaneous compliance with the equilibrium compressibility would show a premature pattern.

Having established that the compression apparatus with its instrumentation was capable of detecting transient effects, we proceeded to investigate the dynamic compression of wood pulp handsheets with the emphasis on dewatering

EXPERIMENTAL

APPARATUS

The compression apparatus (Fig. 1) was described in Report Two. Briefly, the apparatus consisted of a piston movable in a cylinder (3-inch I.D.) mounted on a base plate. The piston was connected with a driving rod through a ball-and-adapter joint. The rod was rigidly attached to the underside of a plunger in an air chamber which was sealed by a rubber diaphragm around the circumference of the plunger. The plunger was forced to move against a spring by compressed air admitted through a solenoid valve. The maximum pressure of the piston is about 700 psi at 100 psi air pressure. All surfaces in contact with the material under compression were smooth except that of the permeable piston which was covered with a coarse and a fine wire screen. The water reservoir in the piston served to keep the material saturated at all times.

The force acting on the piston was measured by a strain-gage load cell mounted between the adapter and the rod. The hydraulic pressure was monitored with a miniature pressure transducer imbedded in the base plate, communicating with the face of the plate through four small water channels. The piston displacement was measured with a linear motion potentiometer. These three signals were transmitted to a multichannel d.c. amplifier and traced optically on a light-sensitive chart. The limit of response was about 0.2 ms (millisecond). All calibrations were linear. The estimated error of the thickness measurement was within ± 0.002 cm, and that of pressure, about $\pm 1\%$.

PROCEDURE

A northern bleached softwood kraft pulp was used in all the experiments to be reported herein. The dry fragments were disintegrated in hot water

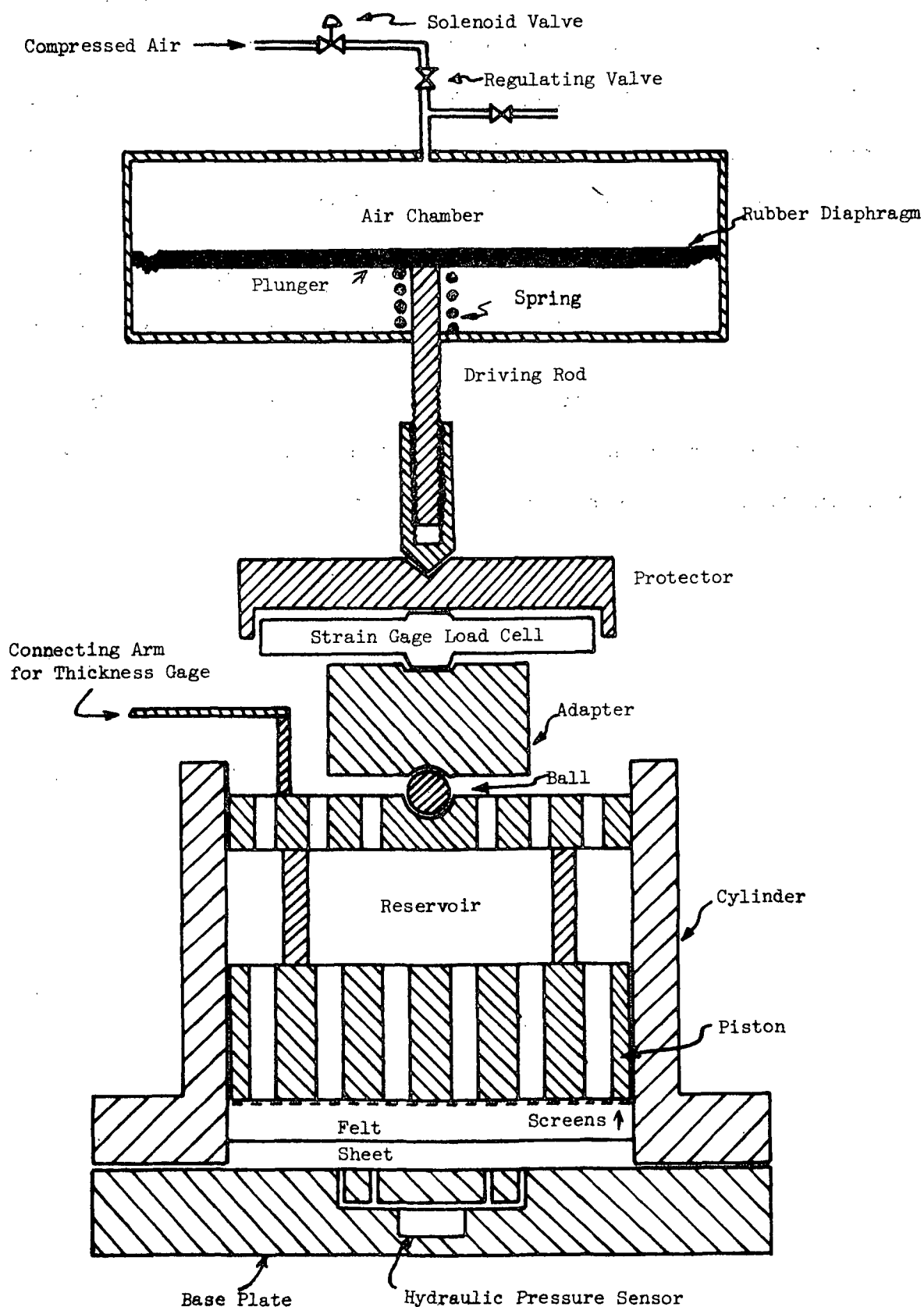


Figure 1. A Sketch of the Compression Apparatus

under a vacuum. The dispersed fiber suspension was formed into a handsheet which was transferred on a felt to the compression apparatus. With the sheet facing the base plate, the piston was lowered gently on the felt. Upon closing the electric switch to open the solenoid valve, a compression test was initiated until it was manually stopped, usually in less than 1 second.

The recorded charts were photographed to yield negative films. The traces in the films were read into digital data with the aid of a microcomparator.

In a static compression test the material was compressed for 15 minutes at a constant load in the same apparatus and the measurements of applied pressure and material thickness were read directly from the instruments.

STATIC COMPRESSION

SHEET

The compressibility of a fiber mat may be expressed by a power function. Refining of a bleached pulp does not affect its compressibility appreciably (1). The data of the handsheets freshly prepared from the original pulp, as well as the lightly refined pulp, were correlated by

$$C = 0.00863 P^{0.266} \quad (1)$$

where C is the sheet density in g/cm³ at the pressure P in dyne/cm² in the test range from 2×10^5 to 5×10^7 , the correlation coefficient being 0.997. This correlation is shown in Fig. 2.

The compressibility so determined in a static test at constant load represents the quasiequilibrium state of the fiber structure, independent of basis weight. It is the ultimate criterion by which the results of dynamic compression may be compared. If the sheet is fully saturated, its water content under compression is related to its density or thickness by

$$\frac{m}{\rho} = \frac{1}{C} - \frac{1}{\rho_f} = \frac{L_s}{W} - \frac{1}{\rho_f} \quad (2)$$

where

m = mass of water/mass of fiber

ρ = density of water, g/cm³

ρ_f = density of fiber (≈ 1.56 g/cm³)

L_s = sheet thickness, cm

W = sheet basis weight, g/cm²

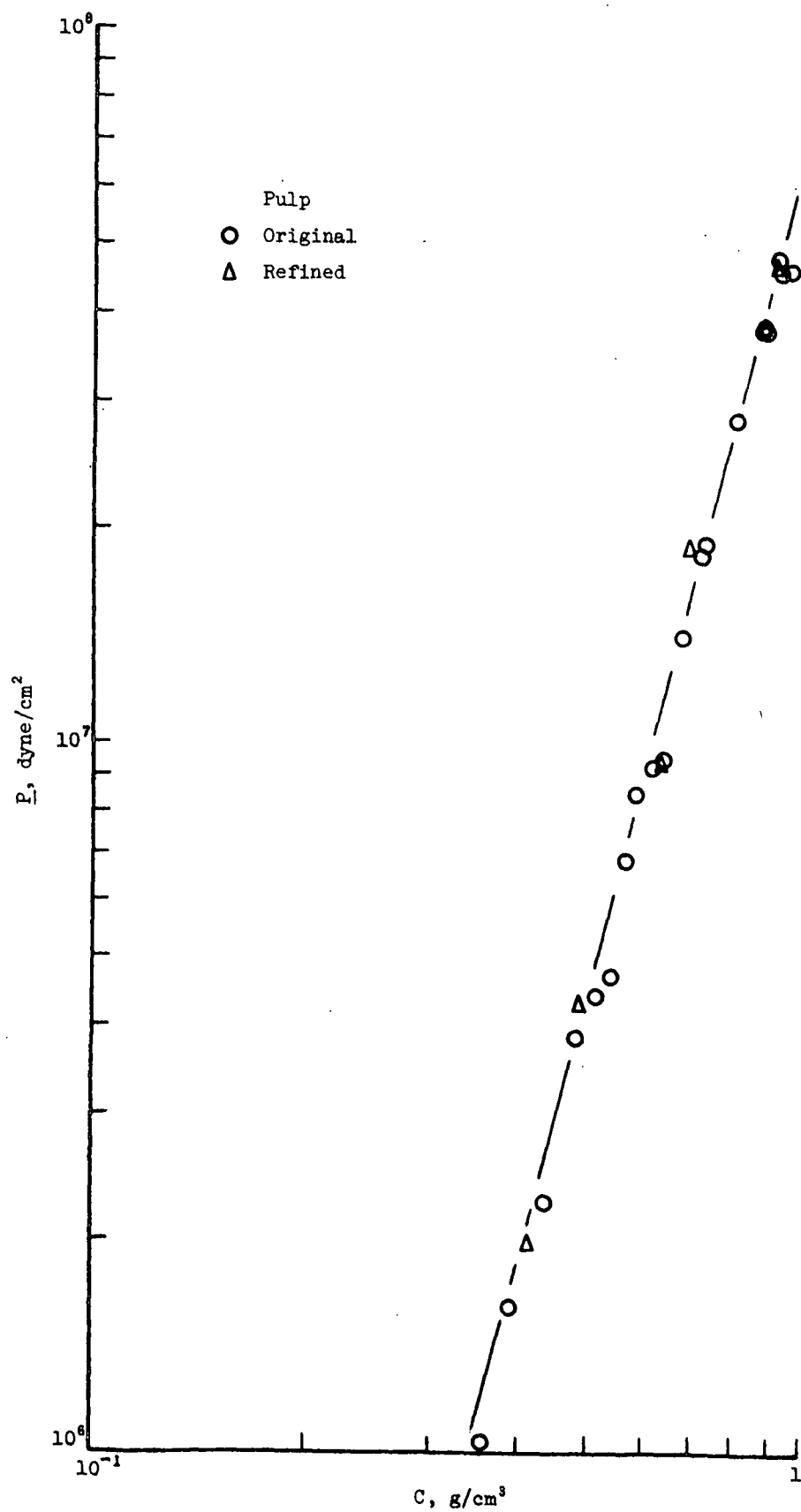


Figure 2. Compressibility of the Bleached Softwood Kraft Pulp

FELT

In the course of the initial experiments it was soon found that the compressibility of the felt samples was not very uniform. Variations among the samples amounted to as much as 12%, as shown in Table I.

TABLE I

FELT COMPRESSIBILITY

Felt Thickness, $\frac{L}{f}$, cm

$P \times 10^{-6}$, dyne/cm ²	Sample					Av.	Stand. Dev.
	1	2	3	4	5		
1.5	0.230	0.241	0.252	0.218	0.244	0.237	0.013
3	0.214	0.225	0.232	0.204	0.230	0.221	0.012
6	0.197	0.208	0.212	0.189	0.214	0.203	0.011
12	0.180	0.195	0.189	0.175	0.197	0.187	0.010
24	0.161	0.172	0.165	0.160	0.179	0.168	0.007
48	0.141	0.152	0.140	0.146	0.160	0.149	0.009

The felt has a woven structure consisting of warps and wefts of highly twisted yarns. Any nonuniformity introduced in the twisting and weaving processes shows up in the finished felt.

When the felt is compressed between two plates, the load is transmitted through the knuckles or yarn intersections and distributed throughout the yarns, the space between the yarns being the least stressed. As the load is increased, the yarns flatten out more, their constituent fibers generate more contact area, and the stresses tend to spread more evenly. This interpretation seems to be consistent with the trend of decreasing variation under increasing load shown in Table I.

Since the stress is concentrated in the knuckle regions, some of the fibers there may suffer irrecoverable deformation, resulting in a slight decrease of the felt thickness at the same pressure when the felt is compressed again. The nonreproducibility of the felt was found to be as much as -5% in thickness for one sample.

SHEET AND FELT

When a sheet and a felt were compressed together, only the total thickness, L_t , was measured. The thickness of the sheet was deduced by subtracting the felt thickness from the total at the same pressure. The sheet thickness so calculated is compared with the sheet compressibility, Equation (1), in Table II. For thick sheets (over 2 g in 45.6 cm²) the agreement is fair. As the sheet weight is reduced, the discrepancy becomes larger and larger. At 0.5 g it amounts to about 50%.

The increasing deviation of the calculated sheet thickness from the compressibility value is largely due to the loss of precision in calculating the difference between two nearly equal numbers. Furthermore, the felt compressibility was always measured after the sheet-felt test, the felt was likely to have slightly lower thickness than in the previous compression. A 5% reduction in the felt thickness is enough to account for a 50% discrepancy for a 0.5 g sheet at high pressures. This explanation, however, does not rule out the various possibilities of sheet-felt interactions in compression, such as stress redistribution due to felt nonuniformity and sheet-felt interfacial structure change.

TABLE II
SHEET-FELT COMPRESSION

$P \times 10^{-6}$, dyne/cm ²	L_t , cm	L_f , cm	$L_t - L_f$, cm	L_s , cm	$(L_t - L_f)/L_s$
Sheet Weight: 3.73 g					
1.54	0.493	0.248	0.245	0.215	1.14
3.56	0.400	0.225	0.175	0.173	1.01
7.32	0.347	0.206	0.141	0.142	0.99
15.0	0.299	0.186	0.113	0.118	0.96
30.5	0.264	0.167	0.097	0.097	1.00
45.9	0.246	0.155	0.091	0.087	<u>1.02</u>
					1.06 av.
Sheet Weight: 2.94 g					
1.20	0.436	0.249	0.187	0.181	1.03
3.90	0.354	0.224	0.130	0.133	0.98
8.29	0.312	0.206	0.106	0.109	0.97
18.3	0.274	0.187	0.087	0.088	0.99
38.1	0.238	0.167	0.071	0.072	0.99
47.8	0.226	0.161	0.065	0.068	<u>0.96</u>
					0.99 av.
Sheet Weight: 1.87 g					
1.62	0.334	0.216	0.118	0.108	1.09
4.06	0.294	0.197	0.097	0.084	1.15
8.62	0.260	0.182	0.078	0.069	1.13
18.6	0.230	0.166	0.064	0.056	1.14
38.7	0.204	0.150	0.054	0.046	1.17
48.0	0.193	0.146	0.047	0.043	<u>1.09</u>
					1.13 av.
Sheet Weight: 1.04 g					
1.01	0.332	0.262	0.070	0.067	1.05
2.19	0.298	0.241	0.057	0.055	1.04
4.55	0.267	0.220	0.047	0.045	1.04
9.30	0.241	0.198	0.043	0.037	1.16
18.9	0.208	0.174	0.034	0.031	1.10
38.2	0.180	0.148	0.032	0.026	1.23
45.9	0.173	0.142	0.031	0.024	<u>1.29</u>
					1.13 av.
Sheet Weight: 0.992 g					
1.36	0.326	0.254	0.072	0.059	1.22
2.67	0.285	0.236	0.049	0.050	0.98
4.40	0.267	0.221	0.046	0.043	1.07
9.25	0.240	0.198	0.042	0.036	1.17
18.9	0.207	0.174	0.033	0.029	1.14
38.2	0.179	0.148	0.031	0.024	1.29
45.9	0.171	0.142	0.029	0.023	<u>1.26</u>
					1.16 av.
Sheet Weight: 0.497 g					
1.54	0.291	0.248	0.043	0.029	1.48
3.47	0.268	0.226	0.042	0.023	1.83
7.32	0.240	0.206	0.034	0.019	1.79
15.0	0.211	0.186	0.025	0.016	1.56
30.5	0.188	0.167	0.021	0.013	1.61
45.9	0.176	0.155	0.021	0.012	<u>1.75</u>
					1.67 av.
Sheet Weight: 0.492 g					
1.45	0.268	0.231	0.037	0.029	1.27
3.76	0.244	0.209	0.035	0.022	1.59
8.34	0.216	0.189	0.027	0.018	1.50
18.4	0.188	0.168	0.020	0.015	1.33
38.2	0.166	0.148	0.018	0.012	1.50
47.3	0.159	0.142	0.017	0.011	<u>1.54</u>
					1.45 av.

DYNAMIC COMPRESSION IN THE PRESENCE OF A FELT

APPLIED PRESSURE

In a dynamic compression test, as the solenoid valve was switched open, compressed air rushed through the throat of the valve at a critical velocity and expanded into the air chamber possibly at a supersonic velocity. Shock waves are, therefore, likely to occur in the very beginning of compression. Figure 3 shows the pressure fluctuations when the air pressure was applied to the piston resting on the stationary plate and when a wet felt sample was compressed. The pressure pulses were practically damped out in about 10 ms.

The data of applied pressure for the first set of handsheets made of the disintegrated pulp at different basis weights are shown in Fig. 4. It is apparent that the time required to reach the preset pressure is longer when the material is more compressible. The rate of pressure rise is governed by the mass flow rate of air, the pressure difference between the supply tank and the air chamber, and the volume of the chamber. When the chamber-tank pressure ratio is below the critical value (≈ 0.53), the throat of the solenoid valve is at the sonic velocity, and the mass flow rate is constant. The rate of pressure rise was found to be proportional to the square root of the tank-chamber pressure difference. At the same chamber pressure, the rate of pressure rise varies inversely with the chamber volume. For a stationary piston the pressure rise is the fastest. For compressible materials the farther the plunger or the piston moves, the slower is the pressure rise.

As discussed in Report Two, the pressure applied to the piston and that borne by the material under test may not be the same. When the piston is accelerating, the pressure acting on the material is less than the measured

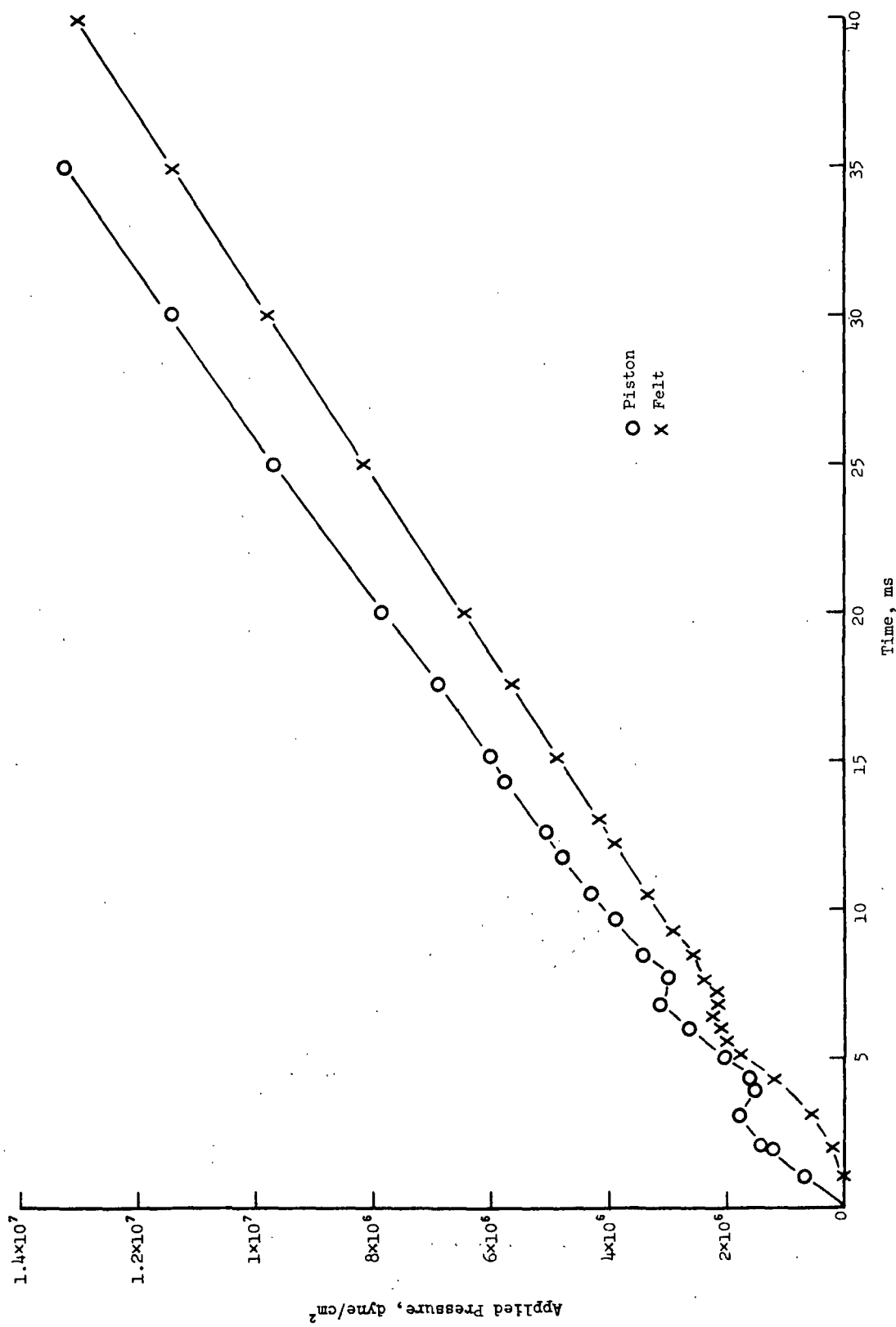


Figure 3. Pressure Oscillations at Early Times of Compression

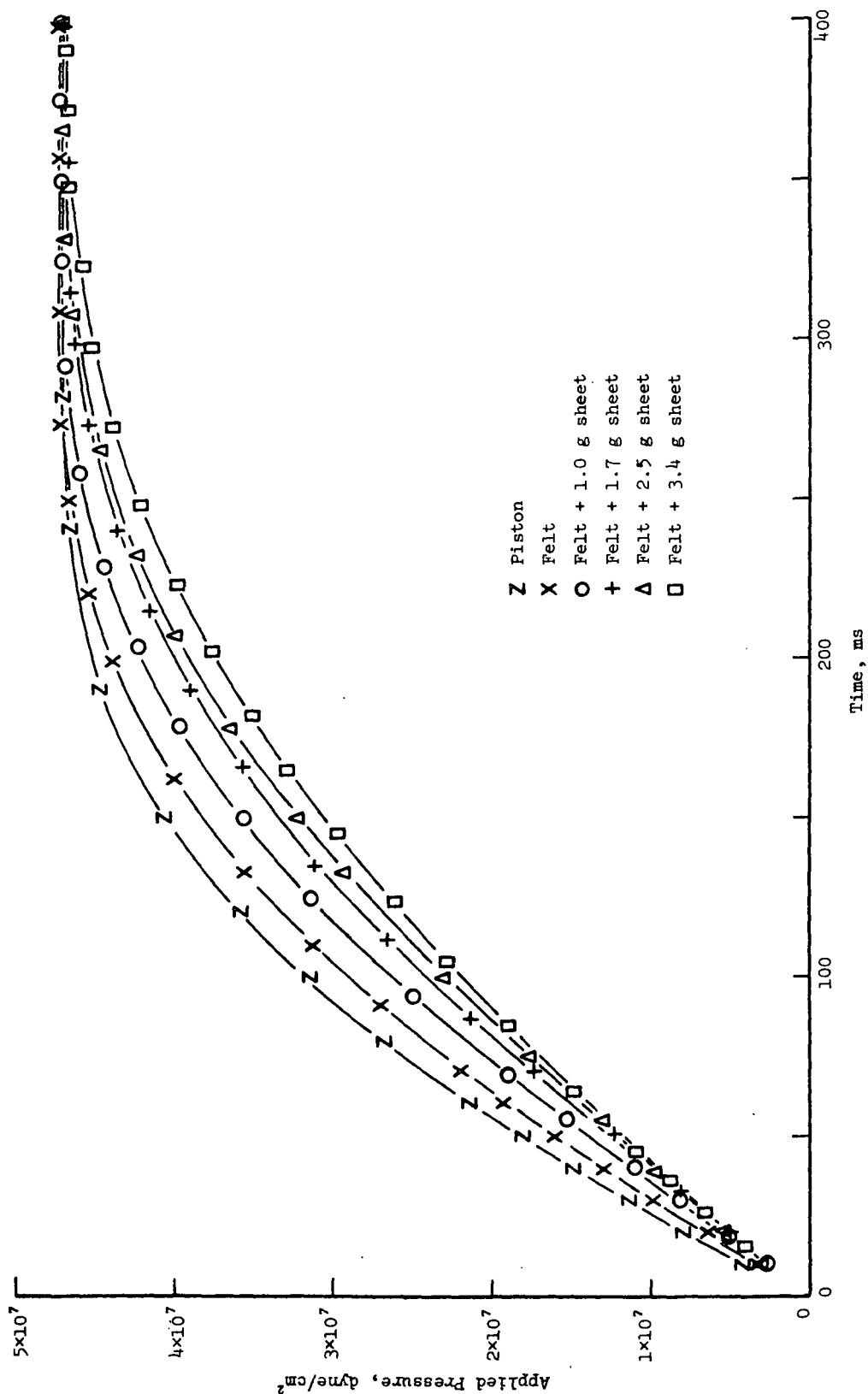


Figure 4. Slow Pressure Rise at Different Basis Weights

value. Conversely, the material experiences a force larger than the apparent load during the piston deceleration. The procedure of pressure correction involves taking graphically the first and second derivatives of the piston displacement. It is a rather laborious task, and incurs a loss of precision. Furthermore, the correction becomes less significant as the pressure rises. From the subsequent discussion of hydraulic pressure it will be seen that the magnitude of correction is up to about 10% of the measured pressure. In this report the pressure correction is omitted.

HYDRAULIC PRESSURE

In the rapid compression of a fibrous material the generation of hydraulic pressure is an indication of the driving force required to overcome the resistance to flow of the fluid relative to the fiber structure. The measured value of hydraulic pressure refers to the pressure drop from the stationary plate across the material to the moving piston at which the atmospheric pressure prevails. It is seen from Fig. 5 that the compression of a wet felt sample alone generates significant hydraulic pressures only in the first few milliseconds beyond which the flow resistance of the felt is negligible compared with those of the handsheets.

Since hydraulic pressure is generated by rapid deformation, its magnitude is limited by the applied pressure. Figure 6 shows a plot of hydraulic pressure vs. applied pressure on log-log scales. The data points in the initial few milliseconds are omitted because of the presence of pressure waves. It is, however, clear that the hydraulic pressure across a sheet develops rapidly to the magnitude of applied pressure within the first 10 ms, during which the piston is initially accelerating. As the piston decelerates,

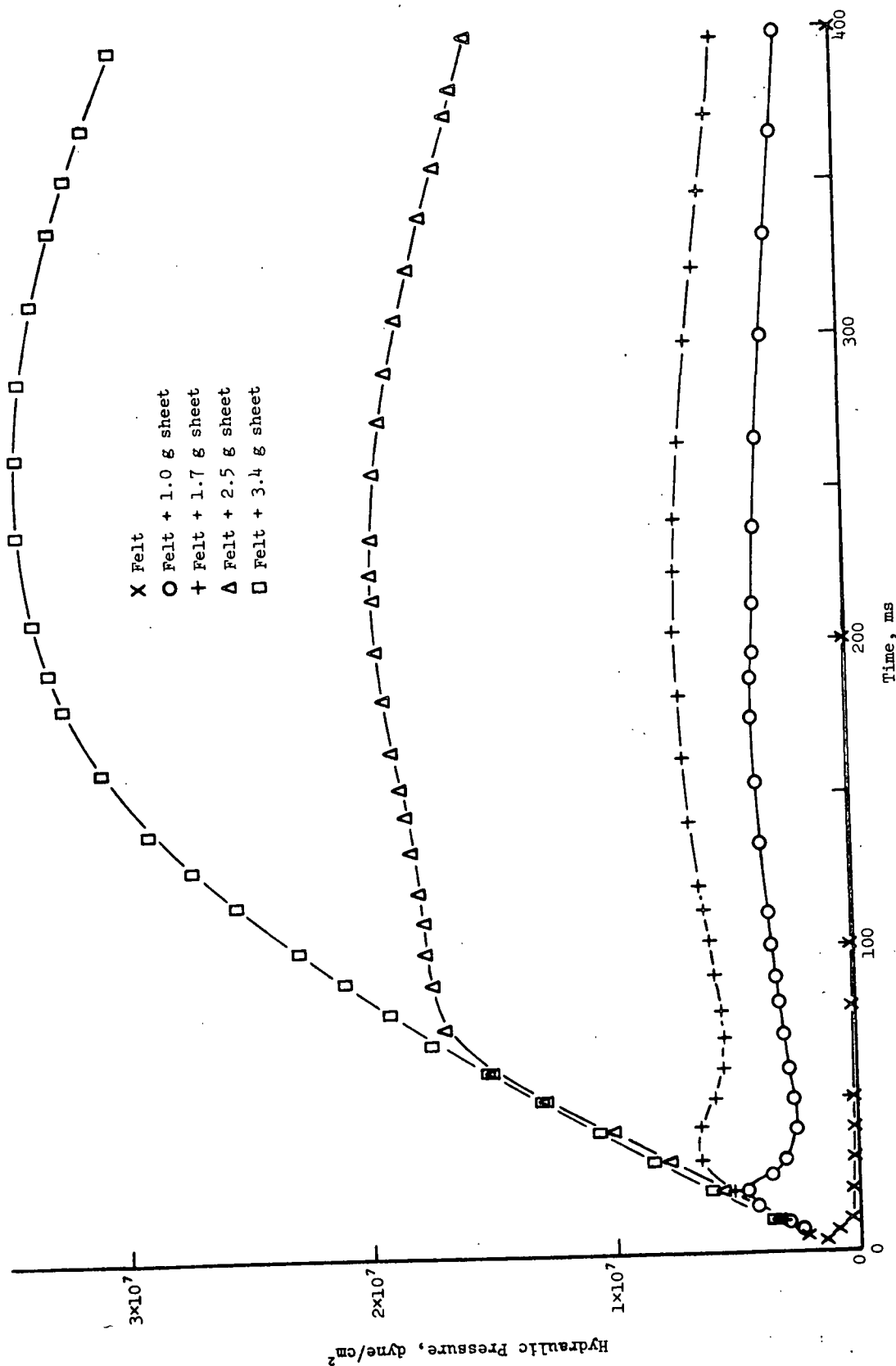


Figure 5. Hydraulic Pressure vs. Time

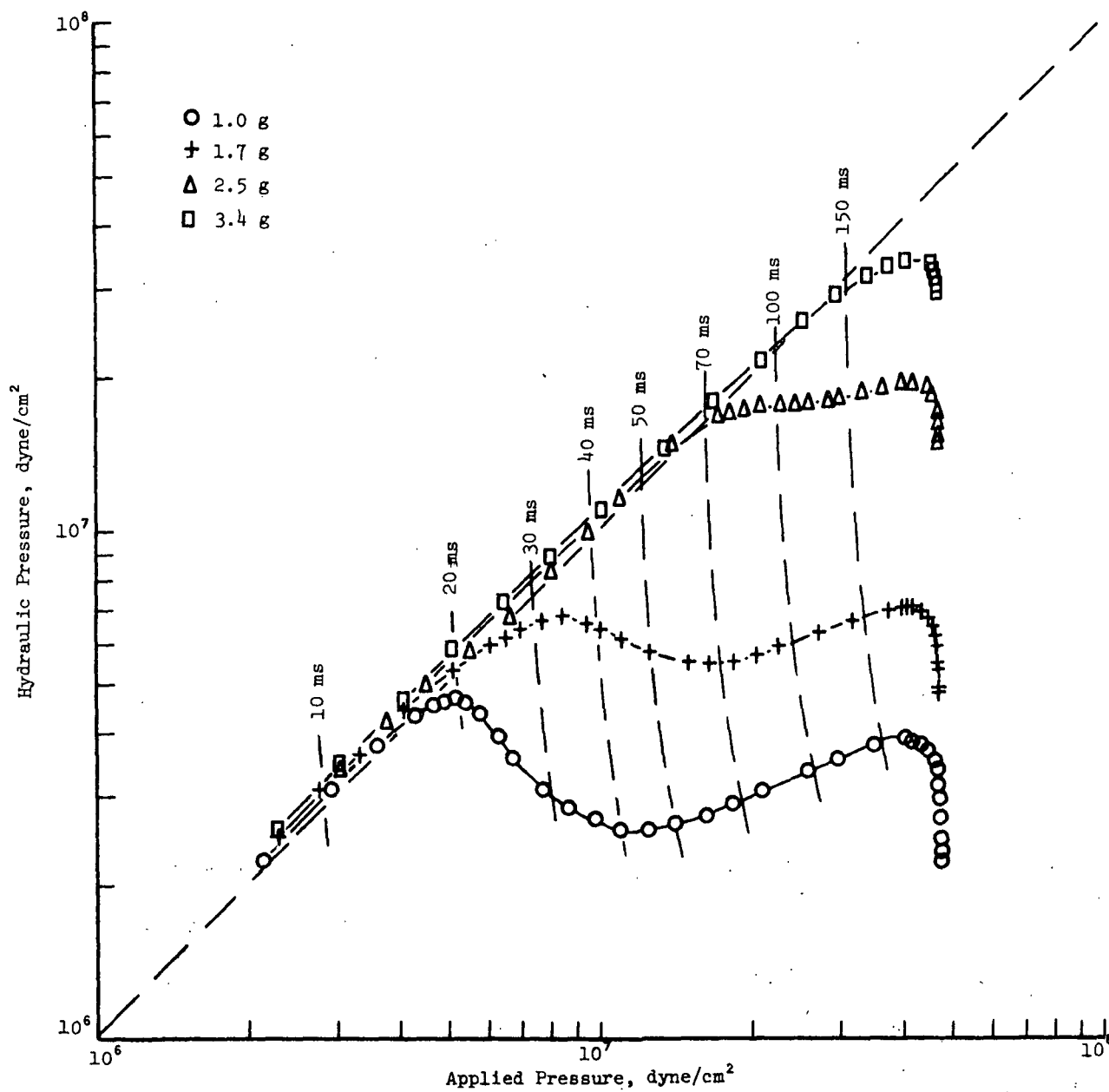


Figure 6. Hydraulic Pressure vs. Applied Pressure

the hydraulic pressure exceeds the measured applied pressure presumably to the extent of pressure correction. The maximum excess is inferred from the data to be about 10% for this series of handsheets.

Figure 6 also shows that after the hydraulic pressure had attained the value of the applied pressure, both rise together for some time which is longer for a heavy sheet. This requires some probing for its implications. Using atmospheric pressure as a reference and neglecting the flow resistance of the felt, the hydraulic pressure at the sheet-felt interface is taken to be zero at all times. In compression of a highly permeable sheet, such as the dacron mat in Report Two, the deformation extends to the whole sheet almost instantaneously, and the hydraulic pressure at the stationary plate registers only a small fraction of the applied pressure. As soon as a substantial amount of water is pressed out, the hydraulic pressure decays rapidly. This may be considered as a case of compressibility-controlled compression (2), in which dewatering is governed mainly by the viscoelastic behavior of the sheet. On the other hand, if the sheet is not very permeable, the compression seems to be initiated at the sheet-felt interfacial layer. Across this layer the hydraulic pressure is generated to accommodate the displacement of water, the remaining part of the sheet being relatively unaffected by the compression. The drag of water over a fiber layer causes the latter to be compressed. As the applied pressure rises, the zone of frictional compression or density stratification expands toward the stationary plate, while the hydraulic pressure drop across the expanding zone remains at the limiting value; i.e., the applied pressure corrected for piston acceleration (the acceleration of the displaced water being negligible). The hydraulic pressure at the front of the zone is transmitted by water to the pressure transducer at the plate. This phase of hydraulic pressure being limited by applied pressure may be called the flow controlled compression.

At the stationary plate there is no movement of water and, therefore, no frictional compression. The layer of the sheet next to the plate is subject to mechanical compression as soon as the applied pressure rises above the hydraulic pressure. The lighter the sheet, the earlier is the point of departure from the diagonal line in Fig. 5. After this point, the hydraulic pressure continues to rise at a rate slower than that of the applied pressure, until a maximum is reached. The maximum occurs at a time when the decrease of the rate of thickness reduction is faster than the increase of the resistance to flow. If the permeability is low, the hydraulic pressure does not decay very fast because as the applied pressure continues to rise, the resistance must increase while the flow is vanishing. The hydraulic pressure is, therefore, a sensitive manifestation of the dynamics of compression. For the same reason it is also liable to disturbances such as pressure pulses and slight unevenness of pressure rise.

SHEET THICKNESS

In the compression test of a handsheet in the presence of a felt, the total thickness of the combined materials is measured as the displacement of the piston. Figure 7 shows the measured thickness for the first series of handsheets and one felt sample. Under the assumptions that (1) the time-dependent compressibility effects of the felt are small, and (2) there is little interaction whatsoever between the felt and the sheet, the sheet thickness may be deduced simply by subtracting the felt thickness from the total thickness at the same pressure.

It is seen that the time lag for the felt becomes larger as the sheet gets heavier and the pressure gets higher. This is a consequence of the slower pressure rise with the heavier sheet. However, the compressibility of a felt changes only mildly with the rate of compression as discussed in Report One.

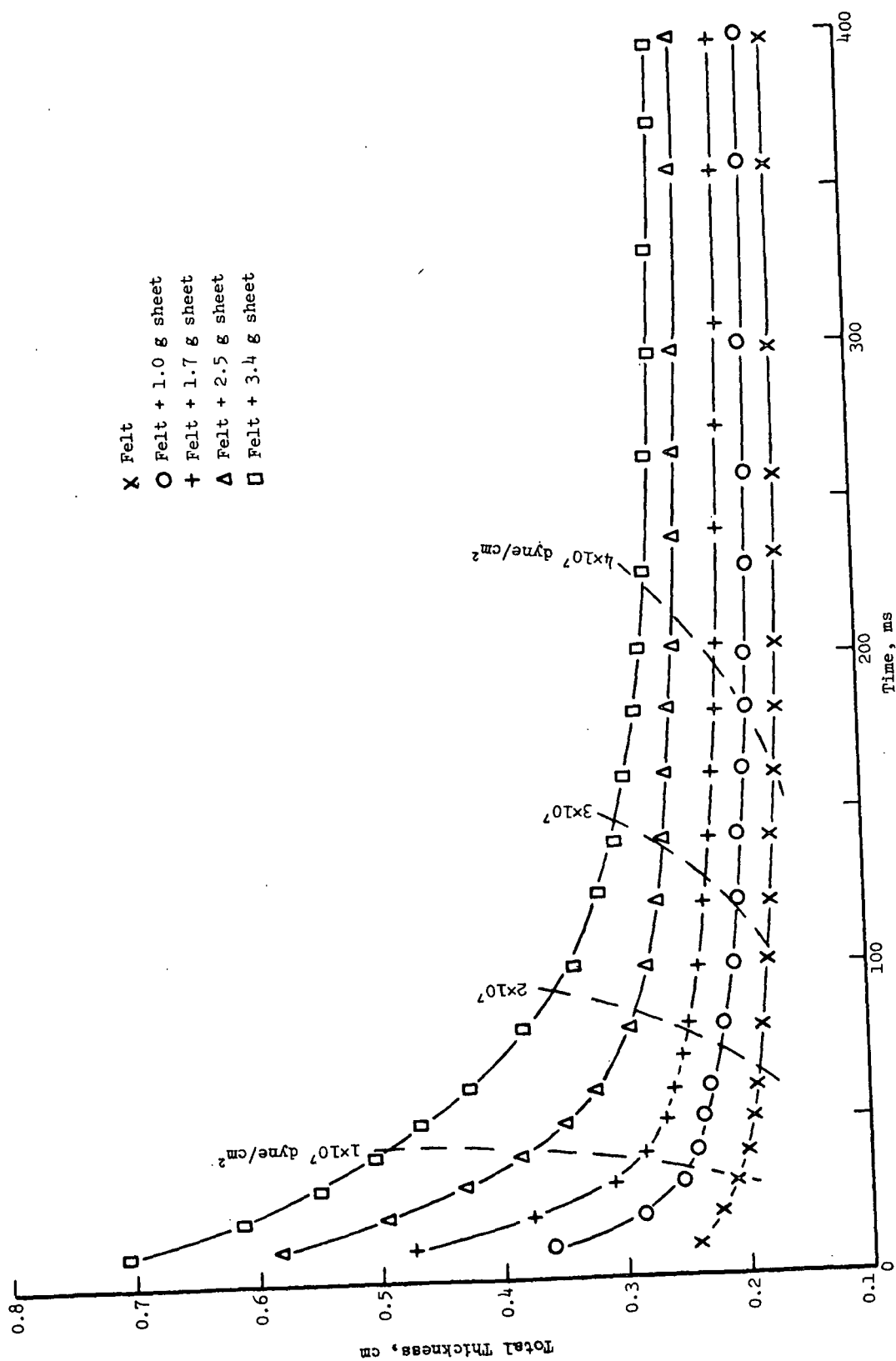


Figure 7. Total Thickness vs. Time

The thickness reduction of a felt in the nip of an experimental press was shown to be inversely proportional to the speed raised to the power of about 0.1. Using this number as a guide, the felt thickness with the heaviest sheet at 4×10^7 dyne/cm² and 220 ms would be 3% smaller than that at the same pressure and 160 ms.

The sheet-felt interactions under dynamic conditions have not been adequately investigated. From the previous discussion of the static compression tests it appears that the direct subtraction is much less justified for thinner sheets.

For the purpose of comparison, the derived sheet thickness for various basis weights is normalized to the sheet density in accordance with Equation (2). The final results for the first series are illustrated in Fig. 8. These preliminary results will not be further discussed because the thickness of the four felt samples used were not individually determined, resulting further in uncertainty of the derived sheet thickness.

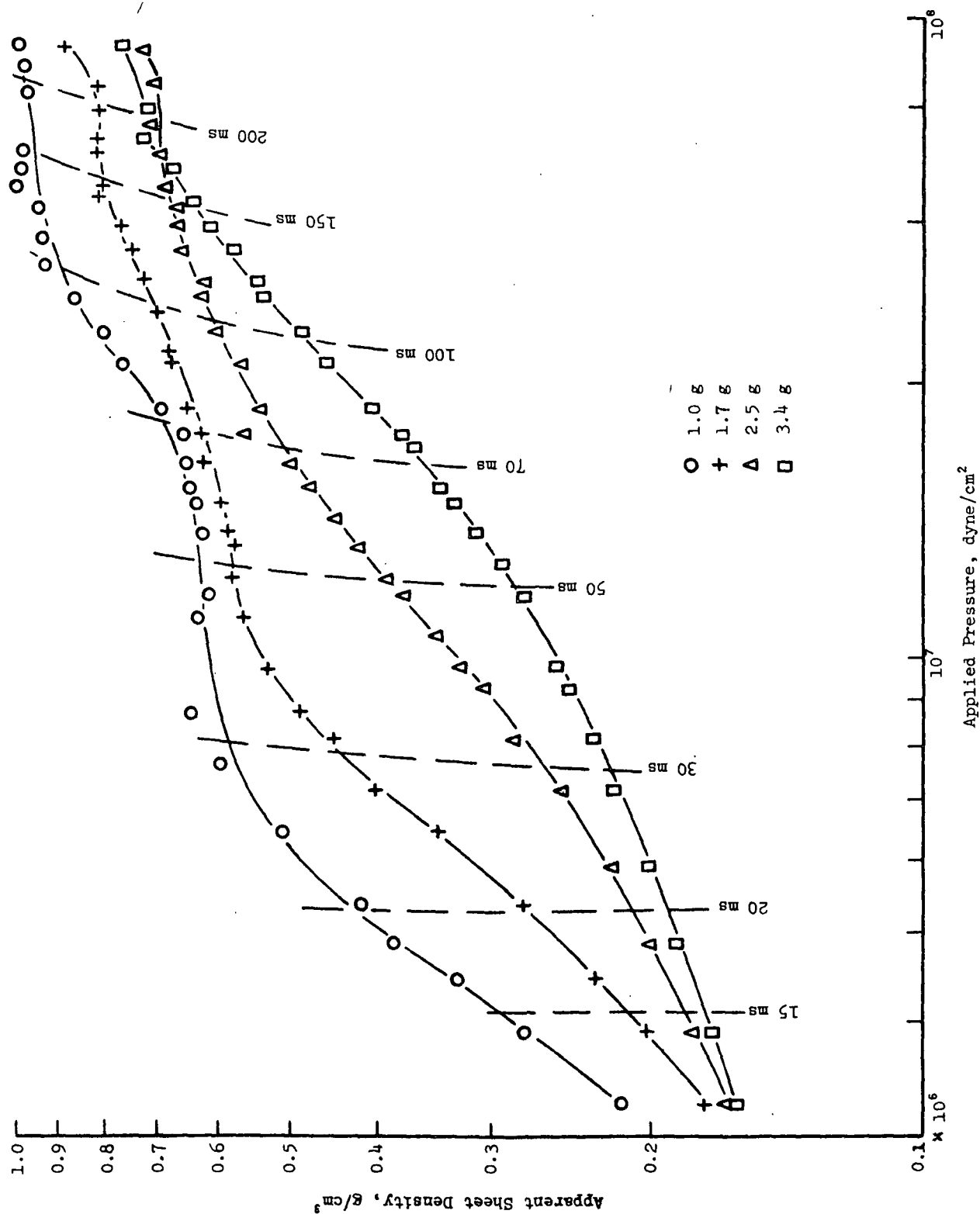


Figure 8. Sheet Density Under Dynamic Compression

DYNAMIC COMPRESSION WITHOUT FELT

PRESSURE SCHEDULE

In view of the uncertainty in determining the thickness of a sheet under compression in the presence of a felt, the succeeding experiments were conducted without any felt. In these experiments there remained, however, a minor complication arising from the deformation of the metallic wire screens at the face of the permeable piston. The screen deformation was found to be significant only at low applied pressures ($< 10^6$ dyne/cm²), necessitating a correction in the sheet thickness.

The original pneumatic driving system allowed the fastest pressure rise to 4.8×10^7 dyne/cm² in about 350 ms. To reduce the compression time the air storage tank, piping, and valves (solenoid and regulating) were enlarged from the nominal 1/4-inch to 1-inch size. The new pressure schedules are shown in Fig. 9 for the compression of 1.7-1.8 g handsheets made of the disintegrated pulp. It is seen that the pressure rise consists of two periods. In the initial period lasting about 30 ms the rise is slow. The low rate is a consequence of an air leak through the solenoid valve while the solenoid is being energized. The leakage is constant and independent of the setting of the regulating valve. The pressure reached in this period depends on the initial pressure imposed on the sheet by hand-adjustment of the piston-plate clearance.

In the second period when the solenoid valve is wide open, the length of time to reach the preset pressure is governed by the setting of the regulating valve. At a given setting the rate of pressure rise decreases as the pressure on the piston approaches the preset value, as previously discussed. The fastest

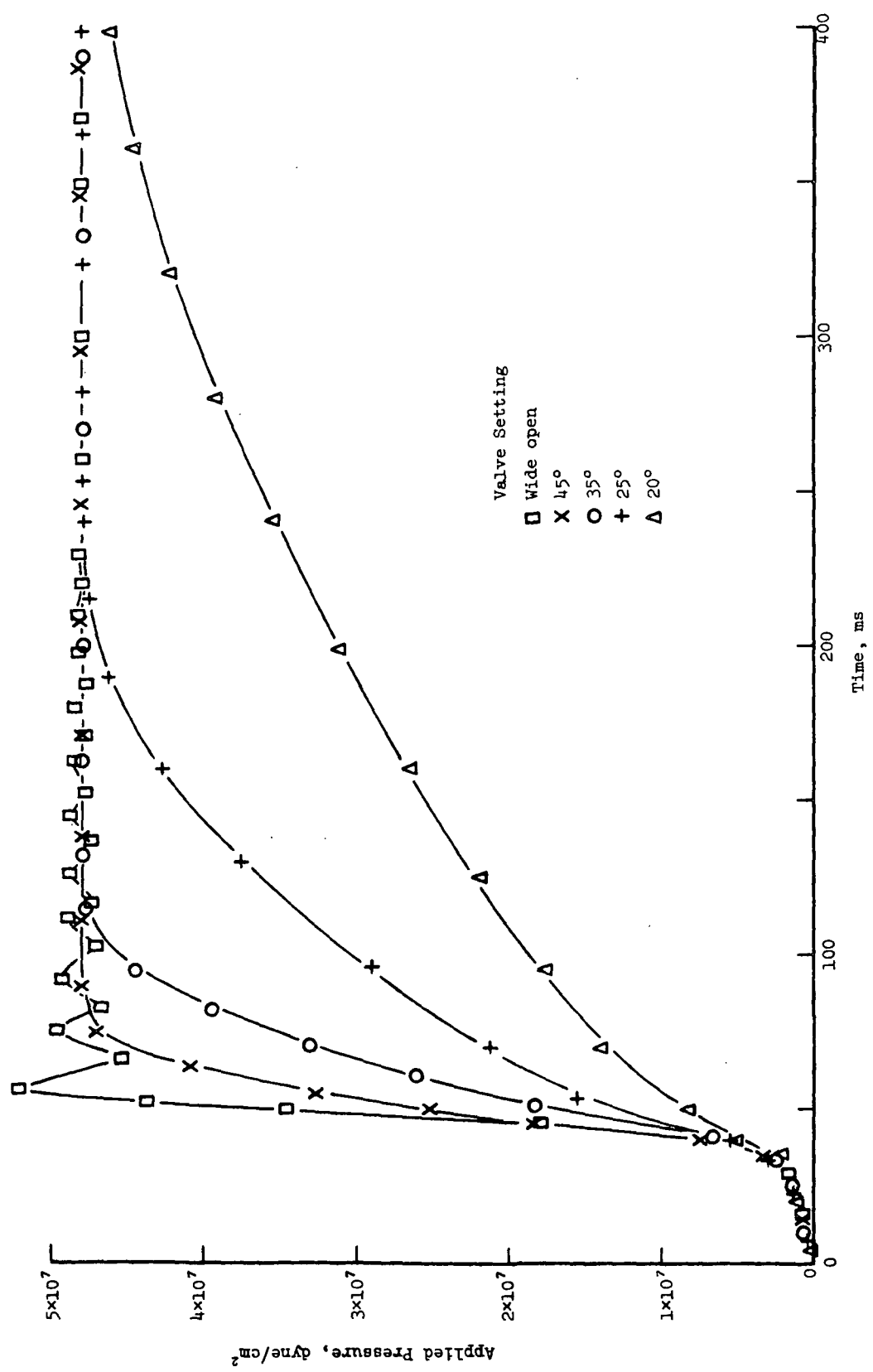


Figure 9. High Rates of Pressure Rise

pressure rise in this period is 24 ms when the regulating valve is wide open. This is barely in the operating range of a commercial press.

At the higher rates of pressure rise the experimental system exhibits under-damped vibration. The pressure oscillates around and decays to the preset value. The oscillation is caused by the impact on the spring-supported plunger in the air chamber, and the damping by the viscous flow of water out of the sheet.

SHEET DEFORMATION

The piston vibration associated with the pressure fluctuation is shown in Fig. 10 for the fastest compression of a 1.7 g sheet. The first 5 or 6 cycles of fluctuations in sheet density are distinct. The exponential decay is partially lost in the creep of the sheet. Mechanical vibration is known to result in a higher sheet density than a steady compression process (1). The effects of frequency and amplitude on dewatering, however, are not yet adequately investigated. In this work we are more interested in the effect of pressure rise on dewatering to be discussed presently.

Figure 11 shows the complete set of compression data for different rates of pressure rise. The upper part depicts the sheet density change in the slow rise period, and the lower part in the fast rise period. In the initial period, the data points are grouped along a band of nearly constant spread. Since the pressure rise is practically the same for all sheets, the spread of sheet density at the same pressure is largely attributed to the difference in the initial sheet density resulting from the piston adjustment. This interpretation is supported by the data pattern as consisting of a family of parallel curves. It appears that at the slow rate of pressure rise the flow resistance is small, and the sheets are compressed almost uniformly. In other words, the percent of deformation or

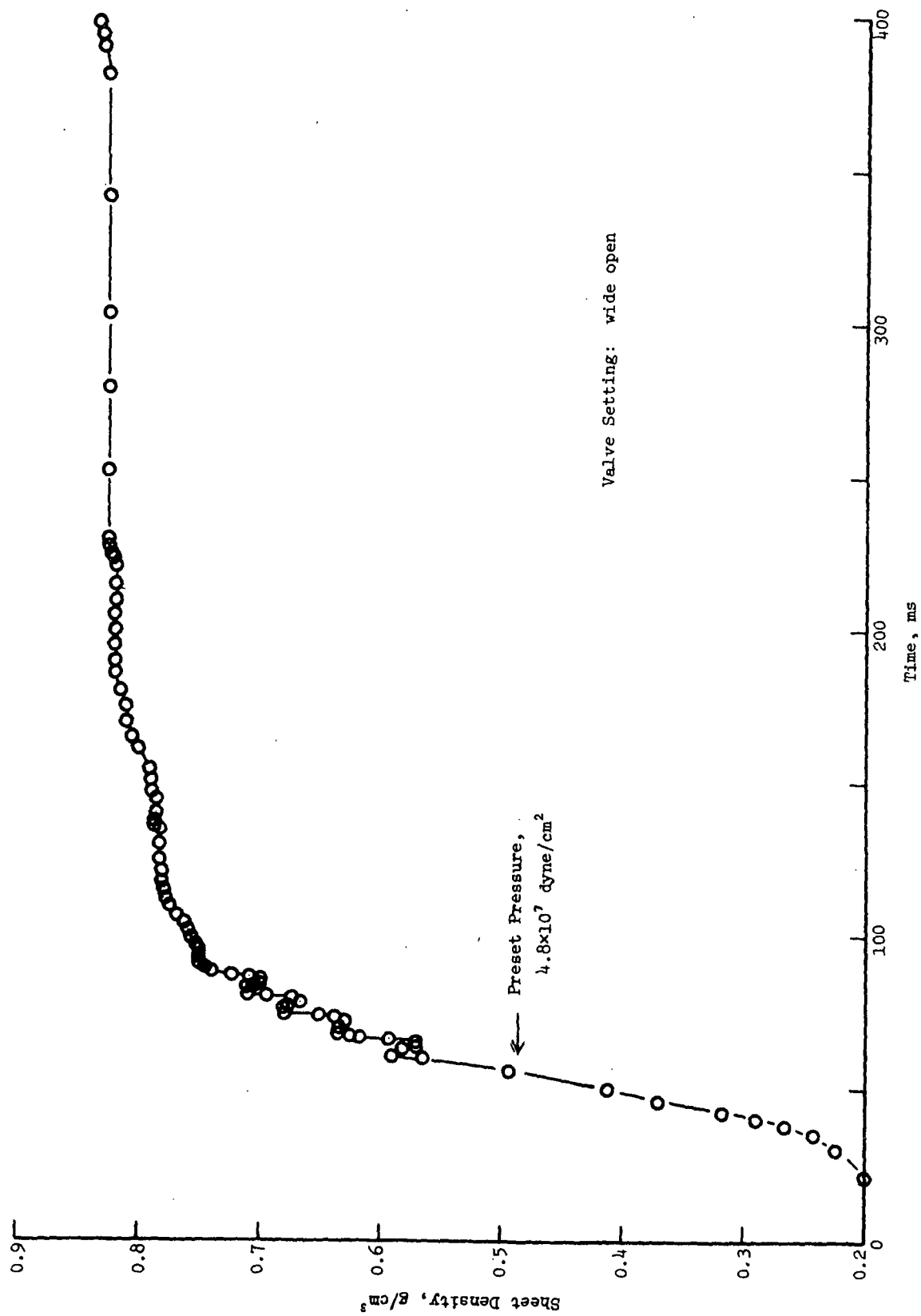


Figure 10. Thickness Fluctuations Associated with Pressure Fluctuations

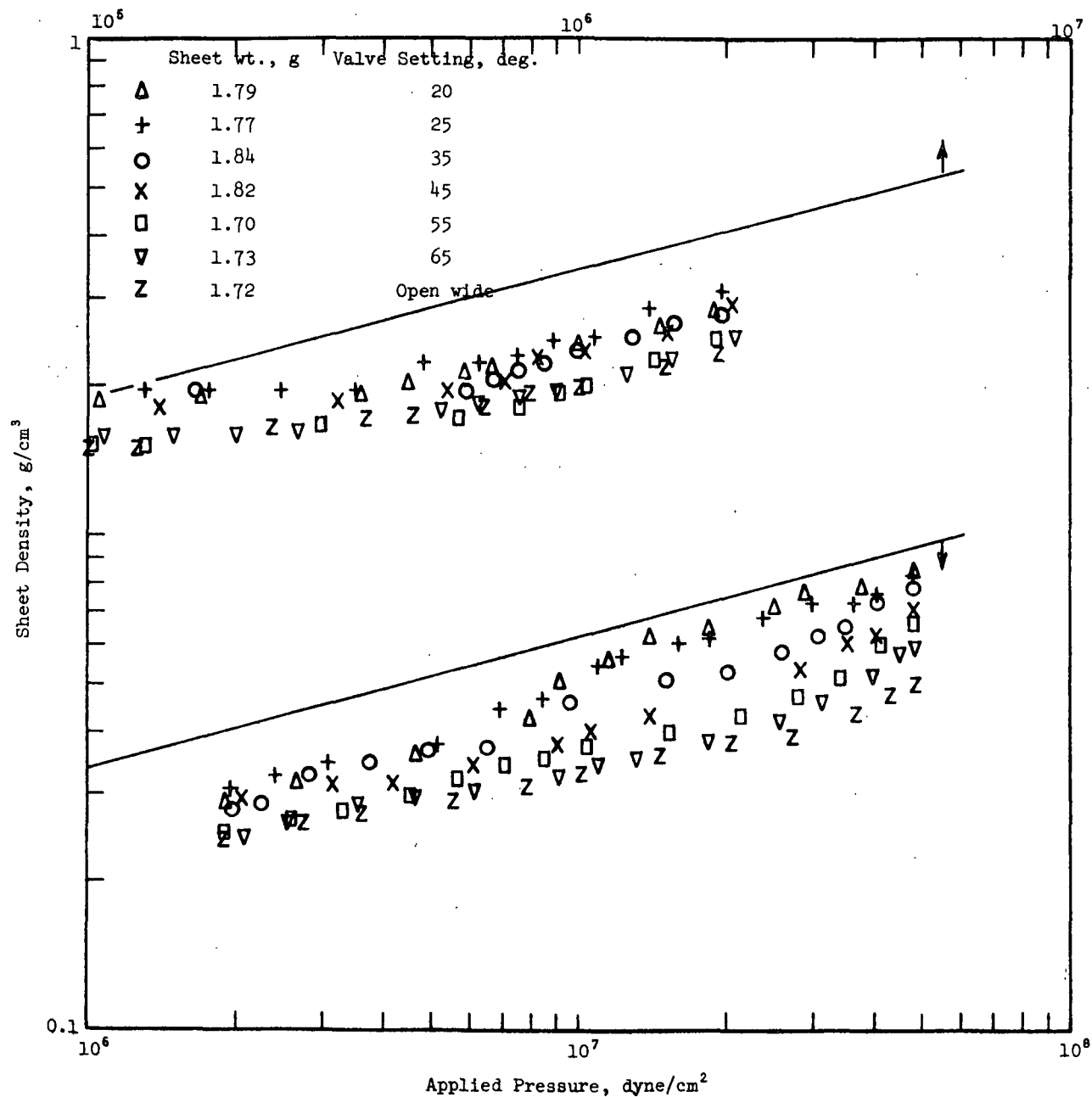


Figure 11. Effect of the Rate of Pressure Rise on Water Removal

strain is about the same for all sheets, a case of compressibility-controlled compression. If the present conclusion is reasonable, the deviation of the dynamic deformation from the static value may be considered as a consequence of the visco-elasticity of the wood fiber sheet structure in response to the short-time (30 ms) compression.

In the subsequent period the data points soon begin to realign according to the time of pressure rise. When the pressure reaches the preset value, the sheet density correlates well with the elapsed time, as summarized in Table III.

TABLE III
EFFECT OF PRESSURE RISE ON DEWATERING

Pulp	disintegrated		
P_1	2×10^6 dyne/cm ²		
P_2	4.8×10^7 dyne/cm ²		
Valve Setting, deg.	Time Elapsed, $t_2 - t_1$, ms	Sheet Weight, g	Sheet Density, ρ_2 , g/cm ³
		static test:	0.941
20	492	1.79	0.835
25	206	1.77	0.816
35	90	1.84	0.789
45	49	1.82	0.705
55	36	1.70	0.650
65	29	1.73	0.604
Wide open	24	1.72	0.493

The same results are more vividly demonstrated in Fig. 12. At low rates of pressure rise the sheet density reached at the preset pressure approaches the static value closely. The continuous increase of deformation under a constant load is referred to as creep. In slow compression the sheet remains nearly uniform, and the extent of dewatering is governed by the sheet compressibility. As the time of pressure rise is shortened, the previously discussed interaction of flow and compression becomes more and more pronounced, resulting in a higher stratification of sheet nonuniformity. In this flow-controlled compression the adverse effect of reducing the compression time on dewatering accelerates rapidly. At very high rates of pressure rise, as well as very high final pressures, it is possible that the interface becomes so dense so quickly that little dewatering is accomplished. Such a hypothetical condition may be described as "interface controlling."

HYDRAULIC PRESSURE

The hydraulic pressure data for the same experiments are shown in Fig. 13, a log-log plot vs. applied pressure. In the initial period of slow pressure rise the hydraulic pressure soon reaches the value of the applied pressure ($< 10^6$ dyne/cm², not shown in the graph). Since the sheet is nearly uniformly pressed at this low rate, a further rise of the applied pressure causes the hydraulic pressure to deviate from the diagonal as previously discussed in connection with the compressibility controlled compression.

In the subsequent fast rise of the applied pressure ($> 2 \times 10^6$ dynes/cm²), the sheet becomes stratified, and the hydraulic pressure rises in parallel to the diagonal until the zone of flow-compression interaction reaches the stationary plate. The faster the rise of the applied pressure, the more stratified is the

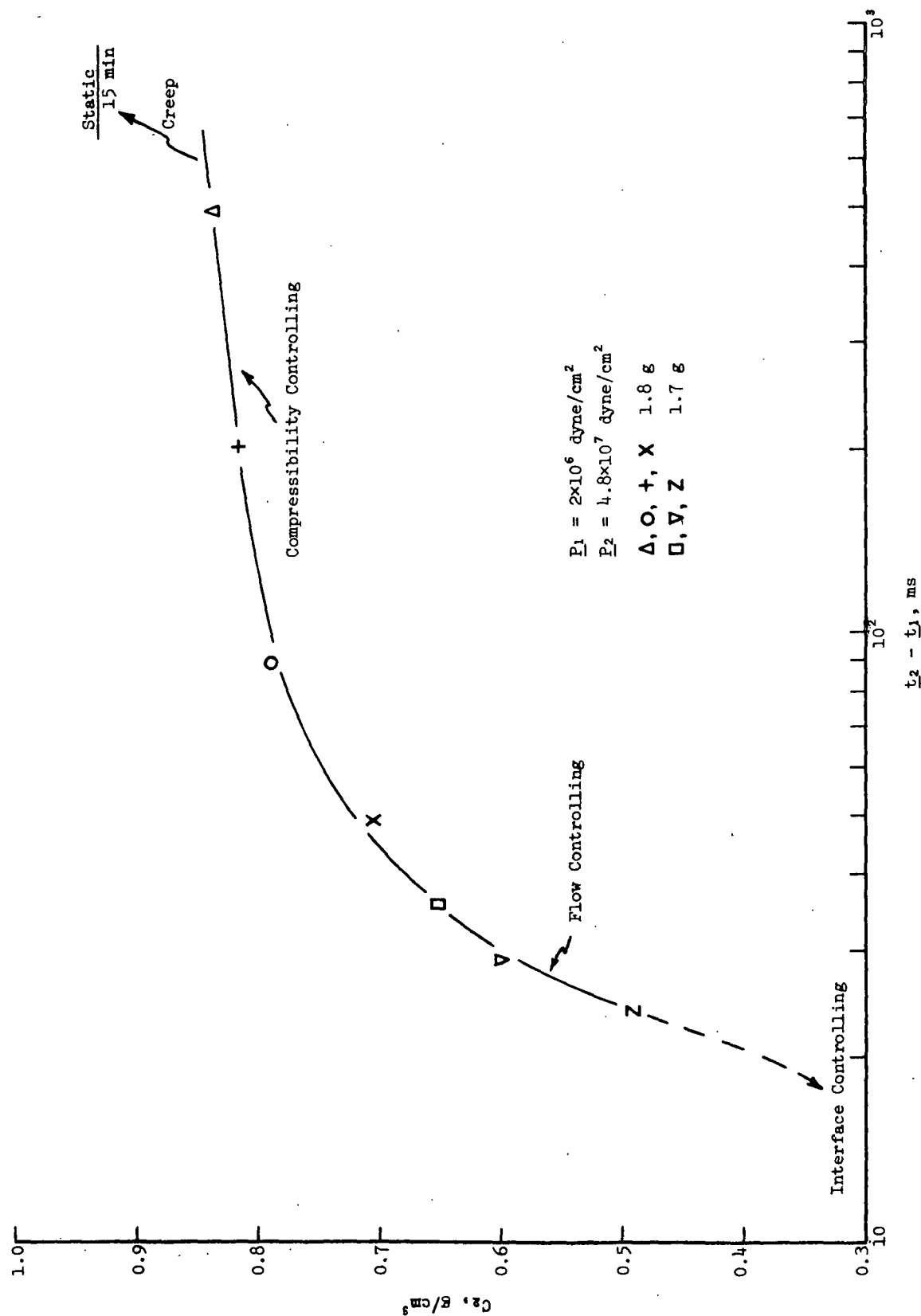


Figure 12. Effect of the Time of Compression on Water Removal

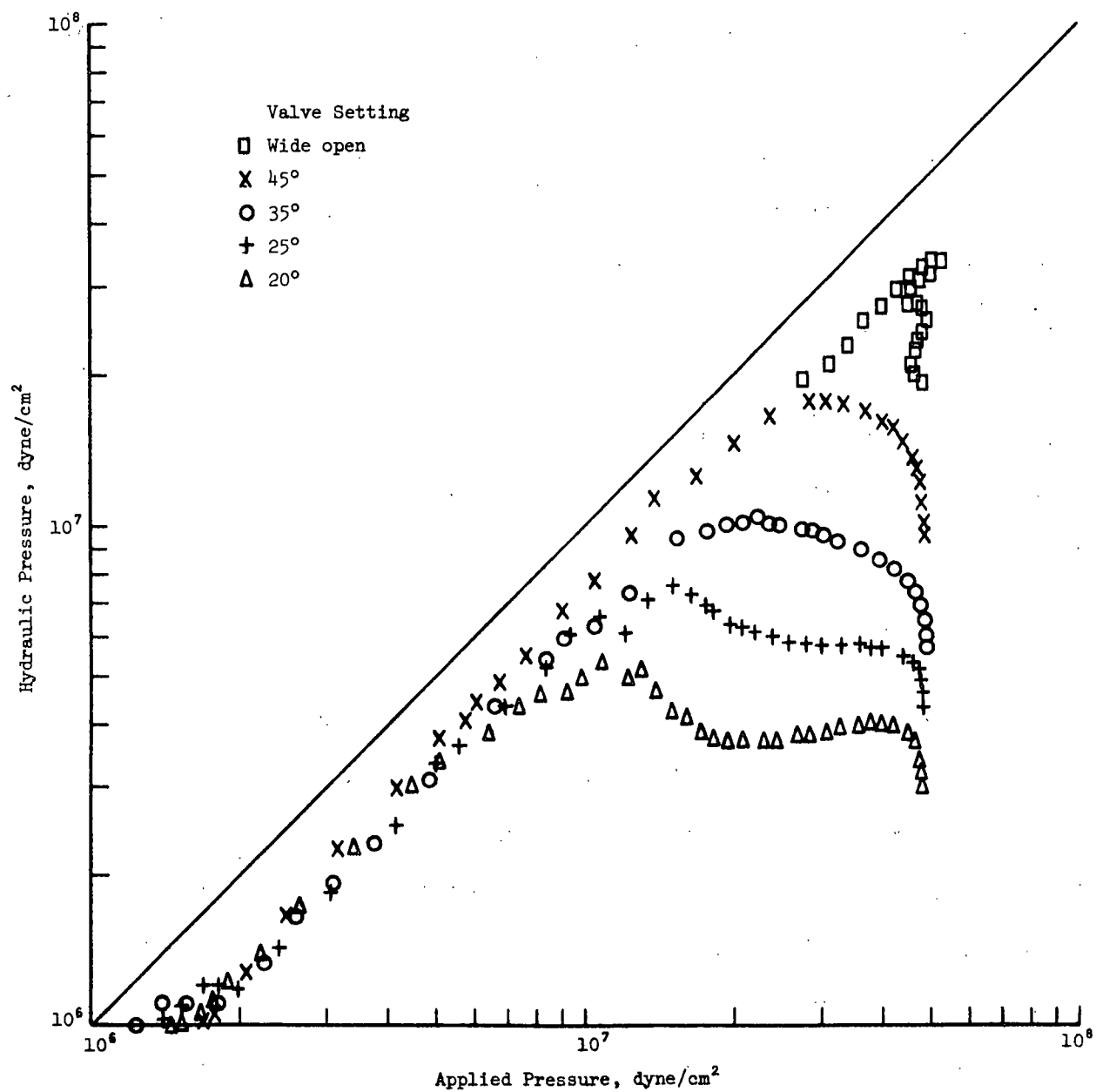


Figure 13. Hydraulic Pressure Under Rapid Compression

sheet. This is consistent with the previous discussion of the flow-controlled compression.

When the applied pressure oscillates about the preset value, the hydraulic pressure falls off steadily, but remains above the atmospheric pressure. Recalling Fig. 10, under pressure oscillations the sheet is responsive to the alternate compression and expansion. In expansion the sheet would reabsorb water from the piston reservoir, and the reverse flow would register a hydraulic pressure below the atmosphere, contrary to the experimental evidence. A possible explanation for this contradiction might be that as the stratified zone at the piston interface expands, water tends to flow both from the piston, as well as the stationary plate into the relaxed zone which is slightly below the atmospheric pressure.

BASIS WEIGHT

The data of a series of experiments with handsheets made of the disintegrated pulp at different basis weights compressed to 4.8×10^7 dyne/cm² with the air regulating valve set at 45° are presented in the next 3 graphs. Figure 14 shows the pressure rise. The slow-rise period is about 35 ms and the fast-rise period, 45 ms. The average rate of pressure rise from 2×10^6 dyne/cm² to the preset pressure, 10^9 dyne/cm²/sec, is closely the same for all the sheets. The hydraulic pressure data in Fig. 15 indicate that the compression of a sufficiently thick sheet (3.8 g) even during the initial slow pressure rise is flow controlled. The sheet is stratified from the beginning, and the zone of stratification has not reached the stationary plate when the applied pressure attains the preset value. The density data are shown in Fig. 16 in separate parts to avoid crowding of the data points.

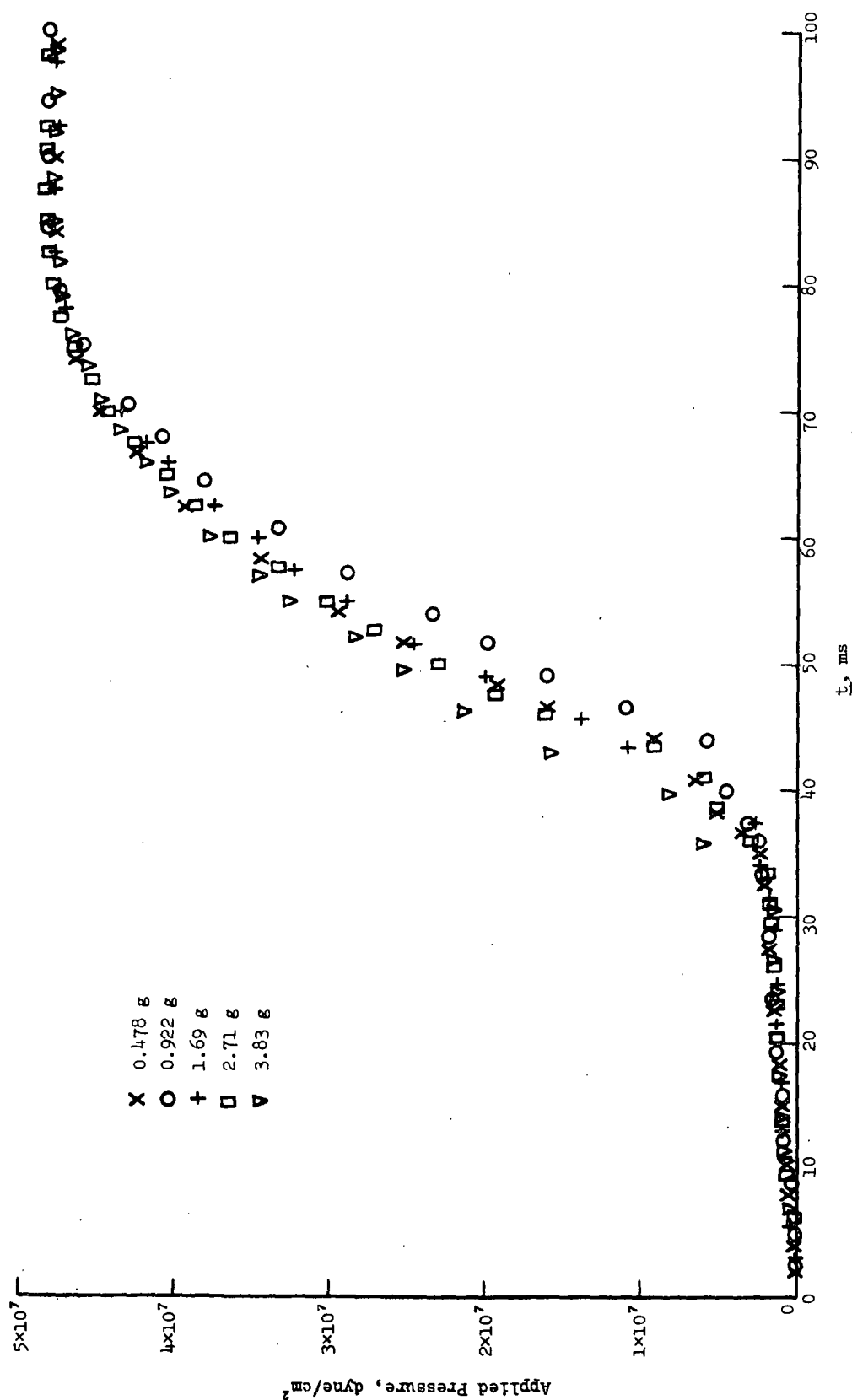


Figure 14. Fast Pressure Rise at Different Basis Weights

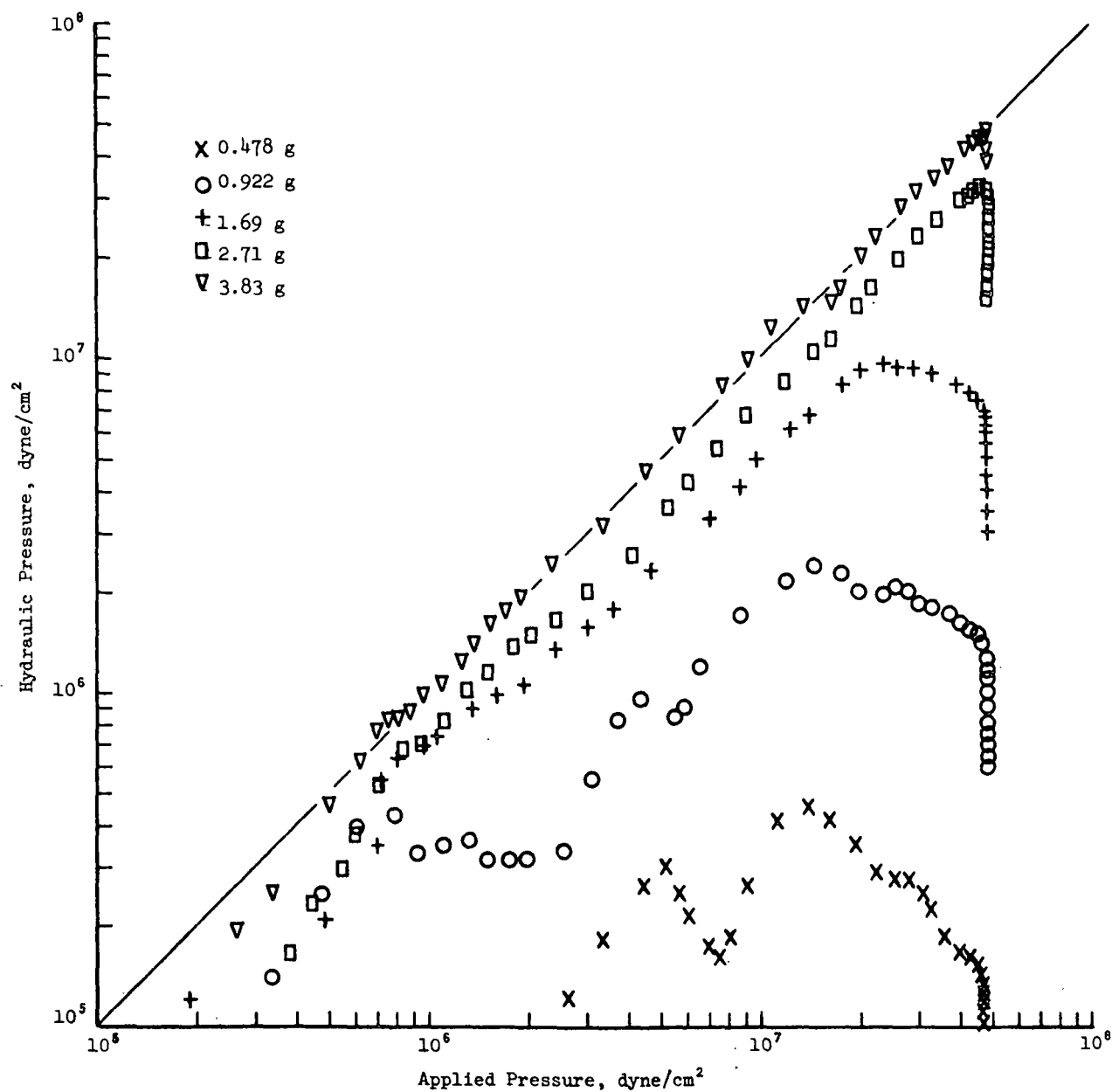


Figure 15. Hydraulic Pressure at Different Basis Weights

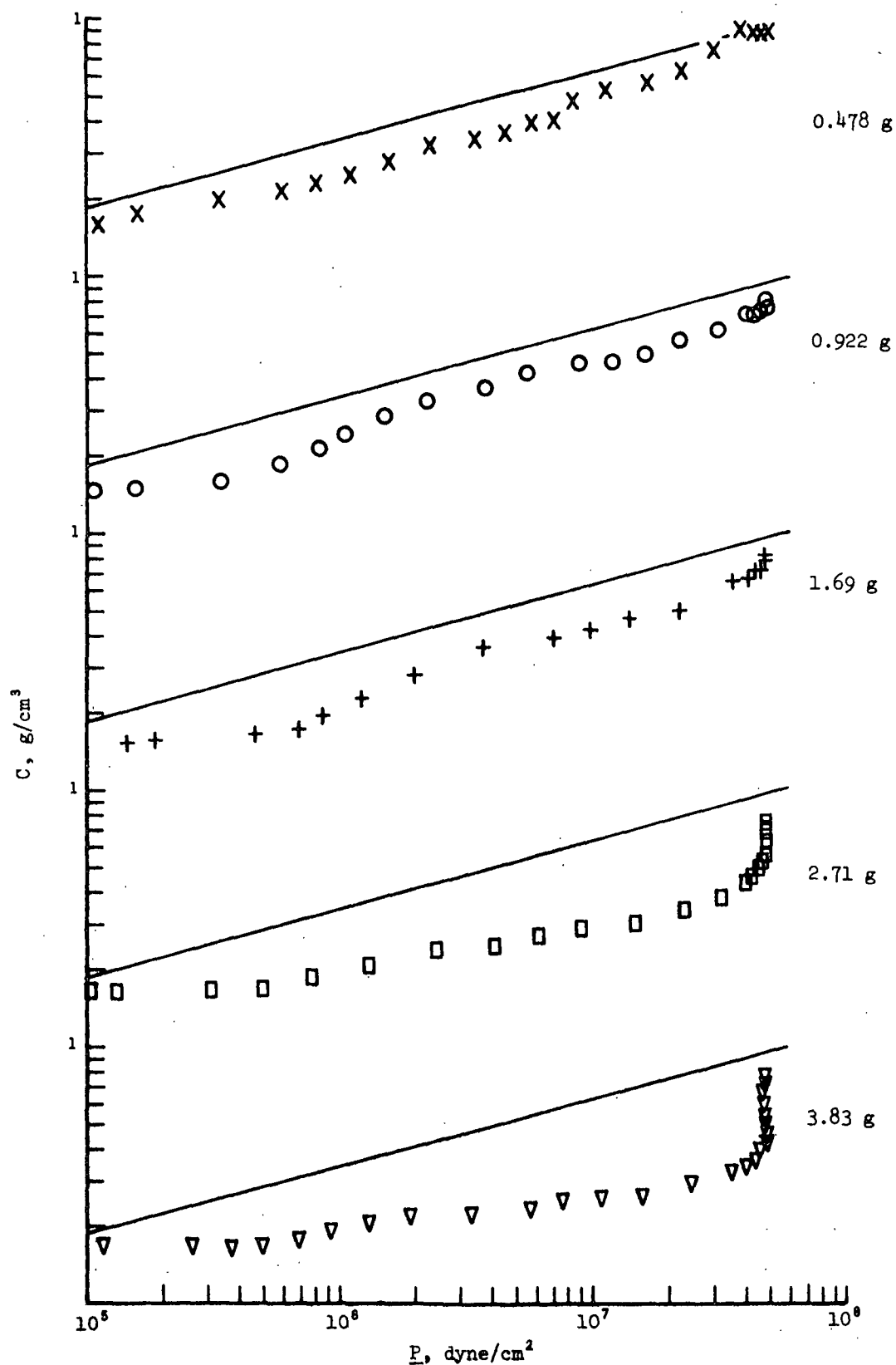


Figure 16. Sheet Density at Different Basis Weights

From these data the effect of basis weight on dewatering is summarized in Table IV.

TABLE IV
EFFECT OF BASIS WEIGHT ON DEWATERING

Pulp	disintegrated
P_1	2×10^6 dyne/cm ²
\bar{P}_2	4.8×10^7 dyne/cm ²
$\bar{t}_2 - \bar{t}_1$	45 ms
Basis Weight, g/m ²	Sheet Density, g/cm ³
Static test	0.941
105	0.874
202	0.758
371	0.751
(400	0.705) ^a
595	0.527
840	0.409

^a() from the previous series.

The results are further plotted in Fig. 17. Under the experimental conditions the compression of thin sheets is compressibility controlled, and that of thick sheets flow controlled.

PULP REFINING

The original, but somewhat aged, pulp after a year's storage was refined in a Valley beater. The lightly refined pulps were made into handsheets at different basis weights, which were tested in the compression apparatus with the air regulating valve set at 45° and the maximum air pressure at 4.8×10^7

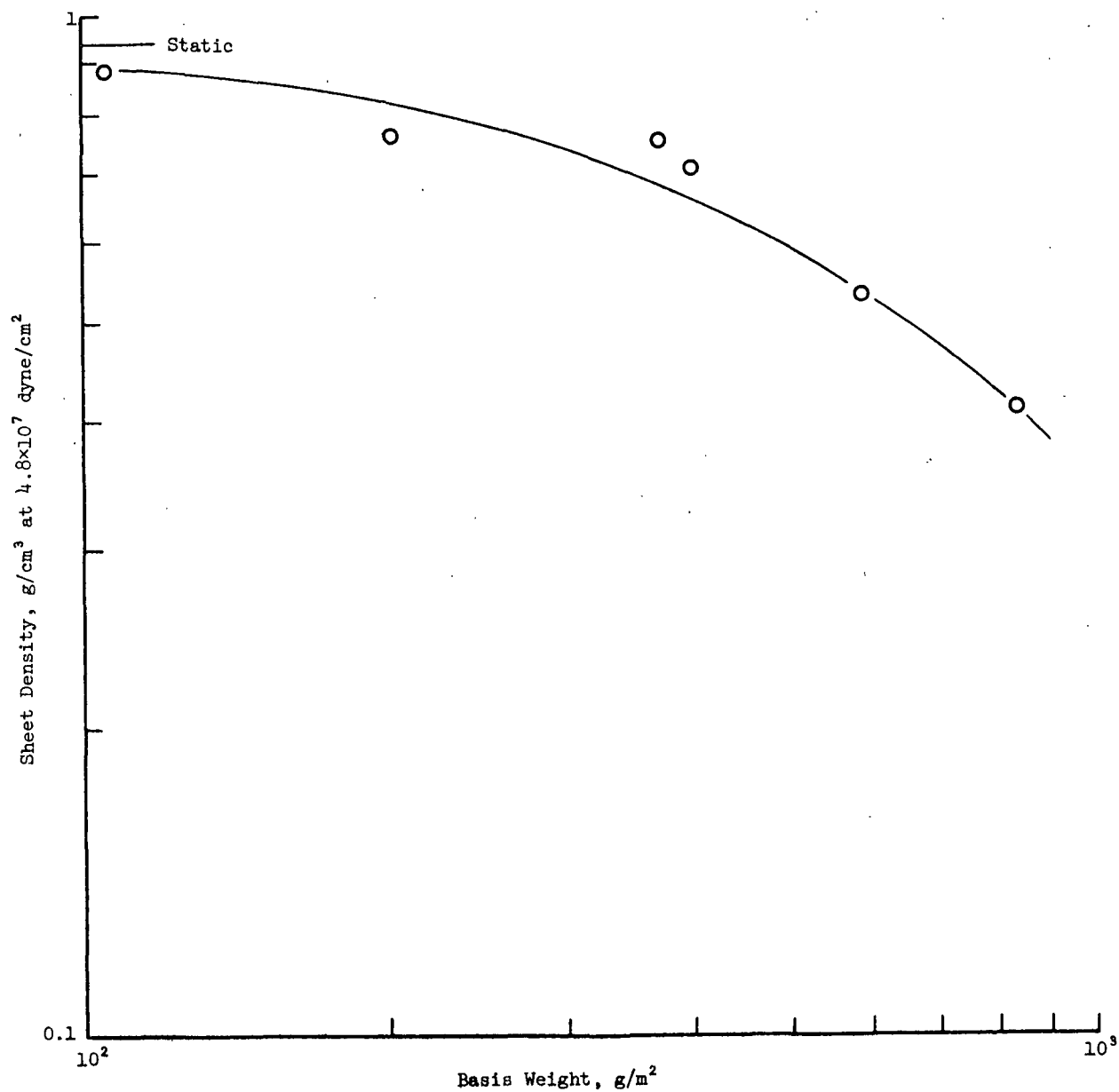


Figure 17. Effect of Basis Weight on Water Removal

dyne/cm². The data for a series of handsheets at 1.8 g are shown in Fig. 18 (applied pressure), Fig. 19 (hydraulic pressure), and Fig. 20 (sheet density). These data are consistent with the previous analysis except that the hydraulic pressure of the refined pulps show considerable higher values than the maximum applied pressures. This could be a phenomenon of resonance, but remains to be verified.

The tentative correlation between sheet density and CSF is illustrated in Fig. 21. It is seen that a small amount of refining affects dewatering drastically under the experimental conditions. A much more meaningful correlation will be the use of permeability which will be determined in the near future. With this information the mathematical model for wet compression may be used for an extensive analysis of the relative effects of the important parameters.

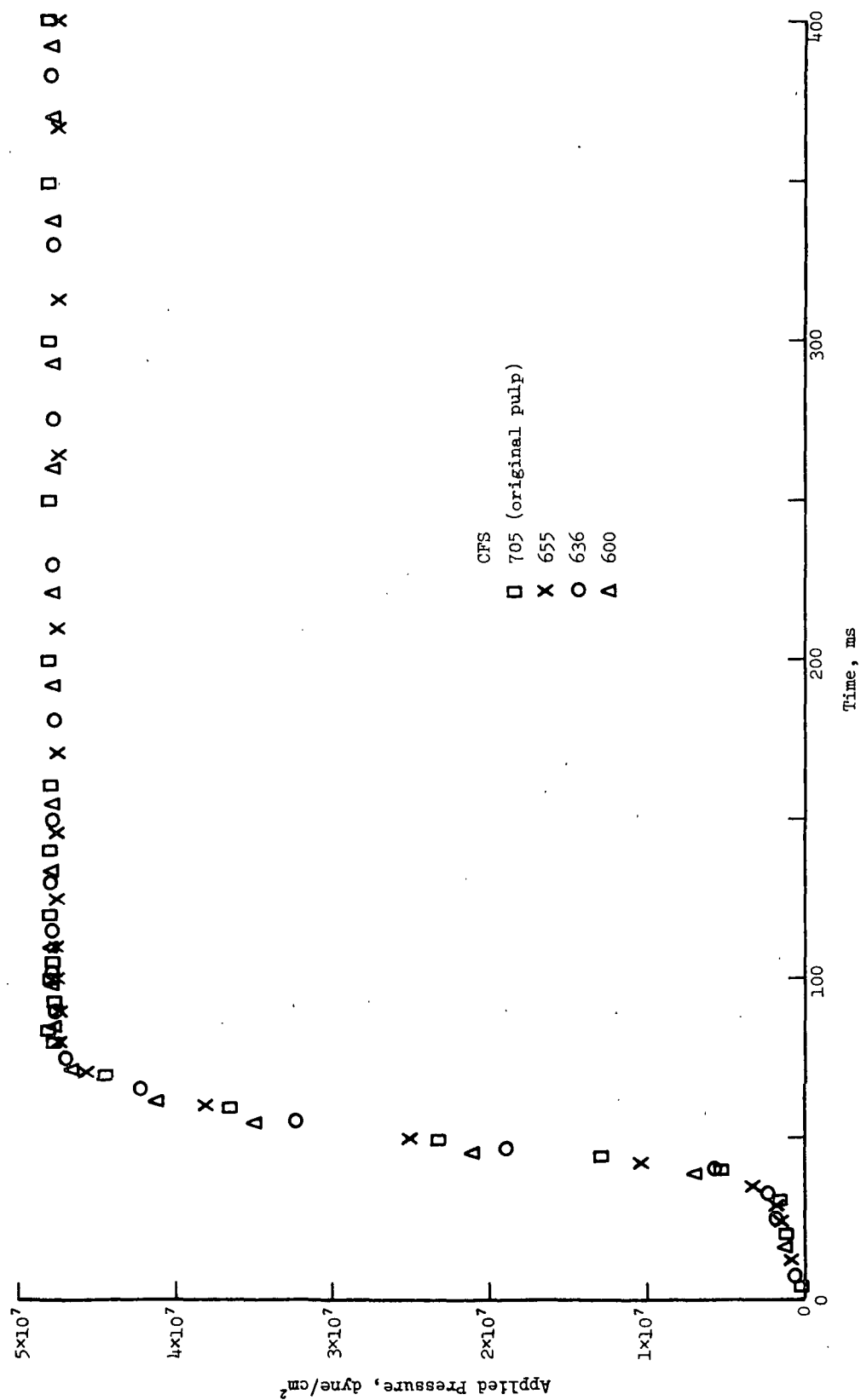


Figure 18. Pressure Rise at Different Freenesses

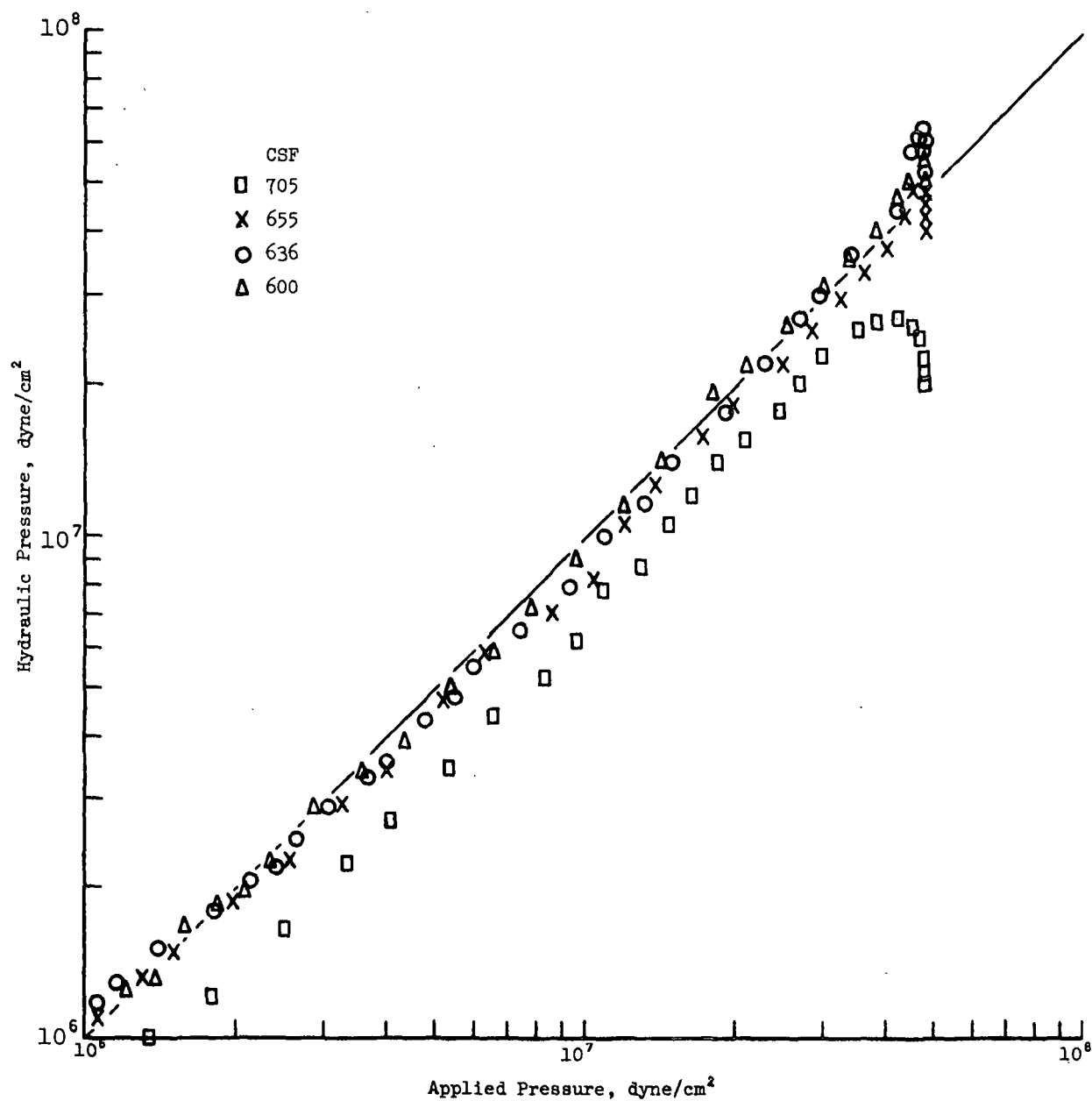


Figure 19. Hydraulic Pressure at Different Freenesses



Figure 20. Sheet Density at Different Freenesses

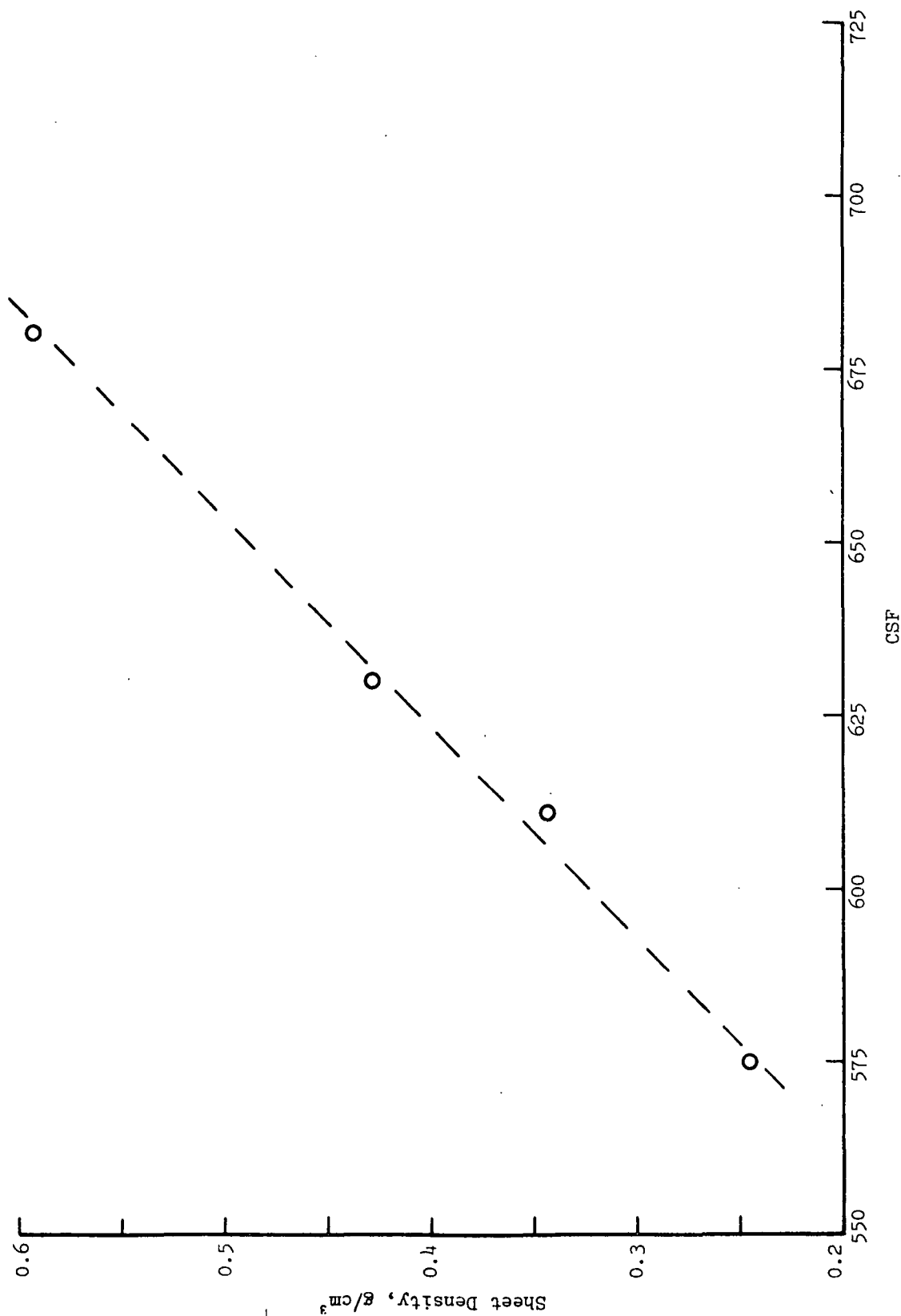


Figure 21. Effect of Freeness on Water Removal

LITERATURE CITED

1. Han, S. T., Pulp Paper Mag. Can. 70(9):65-77(T134-146)(May 2, 1969).
2. Wahlstrom, P. B., Pulp Paper Mag. Can. 70(19):76-96(T349-369)(Oct. 3, 1969).

THE INSTITUTE OF PAPER CHEMISTRY

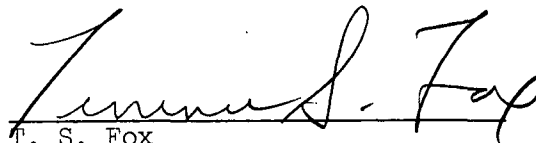


S. T. Han
Senior Research Associate
Engineering Division



Nai L. Chang
Research Associate
Engineering Division

Approved by:



T. S. Fox
Director
Engineering Division

IPST HASELTON LIBRARY



5 0602 01061710 0